INSTITUTE OF PHYSICS PUBLISHING NANOTECHNOLOGY
Nanotechnology **14** (2003) 1153–1160 PII: S0957-4484(03)63490-2

Block copolymer micelle nanolithography

Roman Glass[1], **Martin Möller**[2] **and Joachim P Spatz**[1]

[1] University of Heidelberg, Biophysical Chemistry, Institute for Physical Chemistry, D-69120 Heidelberg, Germany
[2] Deutsches Wollforschungsinstitut an der RWTH Aachen eV, Veltmanplatz 8, D-52062 Aachen, Germany

E-mail: Joachim.Spatz@urz.uni-heidelberg.de

Received 14 May 2003, in final form 1 July 2003
Published 5 September 2003
Online at stacks.iop.org/Nano/14/1153

Abstract
Au-nanoclusters between 2 and 8 nm in diameter were deposited onto solid substrates in different pattern geometries. The basis of this approach is the self-assembly of polystyrene-*b*-poly[2-vinylpyridine ($HAuCl_4$)] diblock copolymer micelles into uniform monomicellar films on solid supports such as Si-wafers or glass cover slips. $HAuCl_4$ as metallic precursor or a single solid Au-nanoparticle caused by reduction of the precursor are embedded in the centre of diblock copolymer micelles. Subsequent hydrogen, oxygen or argon gas plasma treatment of the dry film causes deposition of Au-nanoparticles onto the substrate by entire removal of the polymer. The Au-dot patterns resemble the micellar patterns before the plasma treatment. Separation distances between the dots is controlled by the molecular weight of the diblock copolymers. The limitation of the separation distance between individual dots or the pattern geometry is overcome by combining self-assembly of diblock copolymer micelles with pre-structures formed by photo or e-beam lithography. Capillary forces of a retracting liquid film due to solvent evaporation on the pre-structured substrate push micelles in the corners of these defined topographies. A more direct process is demonstrated by applying monomicellar films as negative e-beam resist. Micelles that are irradiated by electrons are chemically modified and can hardly be dissolved from the substrate while non-exposed micelles can be lifted-off by suitable solvents. This process is also feasible on electrical isolating substrates such as glass cover slips if the monomicellar film is coated in addition with a 5 nm thick conductive layer of carbon before e-beam treatment. The application of cylindrical block copolymer micelles also allows for the formation of 4 nm wide lines which can be 1–50 μm long and also be organized in defined aperiodic structures.

1. Introduction

The field of nanoscience is extremely broad and covers areas from electronics, sensors and healthcare products to micro-electromechanical machines. All these fields are similar in that their functionality is defined by physical or chemical properties, which can be manipulated through the choice of material, material confinement, shape and surrounding matrix [1–5].

A key issue in the fabrication of functional nanostructures is the defined placement and connection of nanometre-sized objects in periodic or aperiodic arrangements on surfaces with different chemical composition and electrical properties.

Principally, there are two major directions scientists follow to address demands from proposed applications in nanosciences, the so-called top–down approach and bottom–up approach. Photolithography and electron-beam (e-beam) lithography are two techniques most frequently used in this technology, which is heavily applied in chip production in the computer industry and employs a variety of very sophisticated lithographic techniques for surface patterning. Different variations of these techniques such as the use of short wavelength light sources, for example deep UV or x-ray, and the chemical adjustment of the polymer resist material to that light sources allowed researchers to keep track with Moore's law [6], which states that the number of transistors squeezed onto a silicon wafer will double every 18 months. Nowadays, structures produced by e-beam lithography, as small as a few nanometres, and photolithography, down to 50 nm, are available. The major drawback of this so-called conventional lithography are large costs caused by tedious fabrication processes and low through put rates for nanometre sized features.

Pure self-assembly techniques provide some means to control feature size even down to a few nanometres and are

practically applicable since the resulting structures are pre-programmed in the molecular structure or colloidal properties. In principle, this technique allows for immense flexibility in terms of the architecture of atom assembly and resulting functionalities. The feature sizes range between 1 and 50 nm. Functionality of the resulting materials is based on material confinement and its assembly into periodic structures with programmed interactions between the building blocks. Self assembly may not cover requirements regarding aperiodic structures or dimensions that are truly greater than 50 nm in terms of feature size and separation distance.

Examination of the potentials involved in the top–down and bottom–up approaches identifies a lack in patterning length scale between 50 and 200 nm regarding object's placement and connection in two or three dimensions. These limitations do not apply for e-beam lithography, however, it is time consuming, expensive and usually covers only small surface areas.

Guided self-assembly provides a more hands-off method to small-scale structuring of aperiodic patterns or structures where nanometre-sized objects are separated by microscopic length scales. Here, self-assembly of molecules guided by chemical or topographical pre-structures allow for symmetry breaking in surface structures and directed location of nanometre-sized features in distinct areas [7, 8]. This biased patterning is based on selective interactions of molecules with pre-structures as well as capillary forces, which cause evaporating solvents to push solvates along the pre-structures. Conventional photo-, e-beam, or scanning force probe lithography are accessible techniques for fabrication of these pre-structures as the length scale is usually larger 200 nm. Guided self-assembly may not account for dense packing of nanowires or dots in aperiodic structures.

A survey of such processes clearly points to the application of micro-contact printing, which has been performed by many scientists. This process allows for fast and reproducible production of chemical micro- and nano-structures with resolutions as good as 50 nm. Smaller dimensions are limited by the contact stability of the stamp with the substrate [9]. Dip-pen nanolithography, the application of a molecular ink using a scanning force probe [10], block copolymer lithography [11–13], colloidal lithography [14], and self-assembled monolayer lithography [15, 16] are additional examples that use clever self-assembly strategies to position and organize molecules into nanoscale structures. Electrochemical modification of self-assembled monolayers at positions where a conductive scanning probe was in contact with a self-assembled monolayer induced a chemical contrast that guided the covalent binding of Au_{55} crystals from solution to surfaces and resulted in lines with widths of less than 3 colloids [17]. Jaeger and Lin [18] demonstrated a method for lateral patterning of metal nanocrystal monolayers in which crystals are protected by a dodecanthiol shell. Extended monolayers of nanocrystals are first self-assembled onto a solid substrate and then immobilized by direct e-beam exposure. During a subsequent washing step, nanocrystals from the unexposed regions are removed, leaving behind the desired pattern. These methods satisfy the needs of most of the current device requirements in nanotechnology.

In summary, there is great potential found in combination of self-assembly approaches and conventional lithographic techniques. Self-assembly guarantees smallest sized features and functionalities programmed in the structure and chemistry of molecules, while conventional lithography meets the demands of controlled structure location of nanostructures with large separation length and also aperiodic arrangements.

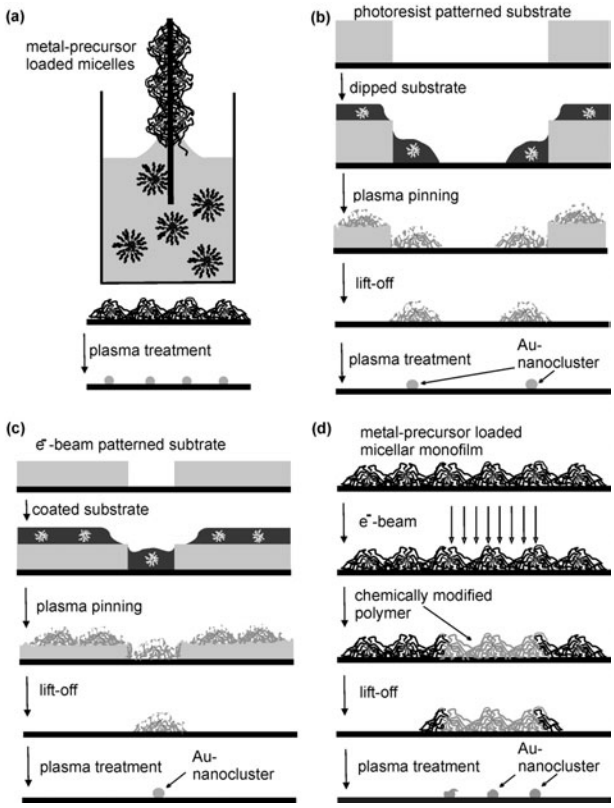

Figure 1. Scheme that summarizes different concepts to nanostructure substrates by block copolymer micelle lithography. (a) Formation of extended monomicellar films and subsequent plasma treatment. Guided self-assembly of block copolymer micelles along pre-structures generated by (b) photo lithography and (c) electron beam lithography. (d) Application of monomicellar films as negative electron beam resist. In (b)–(d), the complementary length scales of a diblock copolymer micelle in which a single nanodot is perfectly positioned in the centre and the resolution of photo- or e-beam lithography which reaches the diameter of a diblock copolymer micelle makes this concept a suitable technology for inexpensive generation of various nanostructure patterns.

The use of macromolecules or structures associated from macromolecules are of special interest in this respect since these allow for bridging the length scale between a few and 200 nm, which link nanostructures to structure sizes available from photo- or e-beam lithography. Self-assembly of block copolymers or mixtures of homopolymers form complex surface structures with nanoscale features. The self-assembled pattern depends on enthalpic and steric interactions between polymer chains, as well as on the interactions of the polymer chains with the solid interface [10, 12, 13, 19, 20]. These interactions are tunable by molecular parameters, which makes it a valuable tool for surface patterning.

2. Results and discussions

In this extended paper we describe the potential of the controlled application of copolymer micelle nanolithography

Table 1. Molecular weights of block copolymers.

Polymer[a] PS(x)-*b*-P2VP(y)	PS Mn[b] (g mol^{-1})	PS Mw/Mn[b]	Block Mn[c] (g mol^{-1})	Block Mw/Mn[c]
190-*b*-190	19 900	1.09	40 900	1.09
500-*b*-270	52 400	1.05	80 500	1.07
990-*b*-385	103 000	1.07	143 500	1.09
1350-*b*-400	140 800	1.11	182 300	1.11

[a] x and y give the numbers of theoretical repeat units as calculated by the initial monomer/initiator feed ratio.

[b] Number average molecular weight and polydispersity of the PS block obtained from size exclusion chromatography (SEC) in tetrahydrofuran (THF) and calibrated to poly(styrene) standards.

[c] Number average molecular weight and polydispersity of the block copolymer obtained from SEC in dimethylacetamide (DMA) and also calibrated to PS standards.

Table 2. Diblock copolymer micellar loading with metal salt $L = HAuCl_4$/P2VP, lateral distances of the resulting Au-clusters and Au-cluster height after plasma treatment.

Diblock copolymer	$L = HAuCl_4$/P2VP	Distance ± standard deviation (nm)	Height (nm)
PS(190)-*b*-P2VP(190)	0.2	28 ± 5	2 ± 1
PS(500)-*b*-P2VP(270)	0.5	58 ± 7	5 ± 1
PS(990)-*b*-P2VP(385)	0.5	73 ± 8	6 ± 1
PS(1350)-*b*-P2VP(400)	0.5	85 ± 9	8 ± 1

for generation of nanostructures on conductive and isolating substrates. Amphiphilic block copolymers of polystyrene (x)-*block*-poly(2-vinylpyridine)(y), PS(x)-*b*-P2VP(y), aggregate to uniform micelles in toluene which is a selective solvent for PS. PS blocks form a shell around the less solvable P2VP blocks to reduce energetically unfavourable interactions with the solvent [21]. The diameter of the micelles is controlled by the molecular weight of the block copolymers and the interactions between the polymer blocks and the blocks with the solvent. The micellar core-shell structure forms a nanoreactor that allows for the selective dissolution of metal precursor salts into the P2VP core or the generation of monodisperse metal particle in each core after an additional chemical reduction step [22]. The particle size is predominantly controlled by the amount of metal precursor added to the micellar solution. Thus, nanometre-sized particles are embedded in a 10–100 nm thick shell of polymer.

2.1. Extended monomicellar films

In this paper, extended and highly regular monomicellar films are prepared by dipping a Si-wafer into a 5 mg ml^{-1} toluene solution of PS(x)-*b*-P2VP(y) diblock copolymers and then retracting the wafer after a few seconds with a speed of 12 mm min^{-1} as shown schematically in figure 1(a). The molecular weights of the diblock copolymers varied according to table 1. In all cases, a part of the 2VP units were neutralized by addition of $HAuCl_4$ to the toluene solution as listed in table 2 and stirring it for at least 48 h, i.e. PS-*b*-P[2VP($HAuCl_4$)$_x$]. After air-evaporating the toluene solvent from the substrate, the monomicellar films were treated with either a H_2-, Ar-, or O_2-plasma that removes the polymer shell entirely as shown by detailed XPS investigations [29]. Then these substrates were investigated with a scanning electron microscope (SEM)[3] as depicted in figures 2(a)–(d). Uniform Au-nanoclusters of 2, 5, 6, or 8 nm are shown on Si-wafers[4]. The plasma treated substrates showed a hexagonal pattern of Au-nanoparticles matching that seen on the micellar monolayers before the plasma treatment. The size of the particles was measured from SEM images as well as from scanning force microscopy (SFM) graphs.

The quality of patterns for each polymer can be discerned by the FT-images. The addition of second order intensity spots for the smaller molecular weight polymers indicates very good organization of the gold nanocrystals that decreases at higher molecular weights. This observed loss in pattern quality for the higher molecular weight polymer micelles arises from the softness of the shell, which increases with the shell thickness, and causes less position precision of the micelles. A summary of a the diblock copolymers, the loading parameter L of $HAuCl_4$, the lateral distances of Au-clusters after hydrogen plasma treatment, and the clusters heights are listed in table 2. From substrate side view images by high resolution transmission electron microscopy as shown in figure 2(e) we know that the Au-clusters are close to spherical shape [7].

So far, block copolymer micelles demonstrate to be a wealthy tool for uniform and extended structuring of solid interfaces with uniform nanometre clusters. While the nanodot size is controlled by the amount of $HAuCl_4$, the distances between nanodots are tuned by the polymer weight of diblock copolymers, where the separation distance can be as large as 150 nm which is the diameter of a micelle in its dry state [23].

[3] The surface characterizations were carried out with a field-emission SEM (FE-SEM, LEO 1530) operating at an acceleration voltage of 1 kV with a beam current of 90 pA or alternatively at 10 kV with 177 pA, as measured with the Faraday-cup.

[4] In a TEPLA E-100.

2.2. Guided self-assembly: organization of block copolymer micelles along lithographic pre-structures

In order to arrange nanoparticles in an aperiodic structure or to separate individual nanoparticles at distances greater than the resolution of conventional optical microscopes, that is more than 250 nm, block copolymer micelles loaded with individual nanoparticles or with the respective metallic precursor are positioned along a topographically defined pre-structure. Such a pre-structure can be fabricated by standard photo or e-beam lithography as shown schematically in figures 1(b) and (c).

In figure 1(b), the use of photo lithography in combination with self-assembly of diblock copolymer micelles is drawn schematically. Photolithography was processed according to standard procedures described by Allresist (photoresist X AR-P 7400/8). A Ni-mask with holes of 4.5 μm diameter separated by 2.5 μm were used to illuminate the resist partly with UV-light. Developing of the resists resulted in grooves with a 4.5 μm diameter and a hole depth of approximately 250 nm which was the original resist thickness. On top of this pre-structure a 0.1 mg ml^{-1} concentrated block copolymer solution of PS(1350)-*b*-P[2VP($HAuCl_4$)$_{0.5}$](400) was spin coated by depositing a few drops on the rotating substrate (10.000 rpm). The resist was carefully chosen so that the interaction between the toluene solvent of the micellar solution and the resist was minimized as was the time the solvent remained in contact with the substrate. The micelles were positioned along the resist borderline due to capillary forces of the retracting liquid film when solvent evaporated. Then, the pre-structured substrates with the deposited micelles were transferred to the gas plasma chamber in order to pre-etch the polymer shell around the metal precursor (100 W, 0.4 mbar, 3 min). Because of this chemical modification of the diblock copolymer the micelles were pinned to the substrate. Pre-etch also corroded the resist film. Since the resist thickness is larger than the shell which is surrounding the metallic precursor immobilisation of partly destructed micelles on the substrate and resist was observed. Under these condition a major part of the resist was still present and could be lifted-off the substrate by aceton. This lift-off removed micelles that were located on top of the resist and not in contact with the substrate. After drying the substrate it was transferred to the plasma chamber once again. Now, either an oxygen or a hydrogen plasma was applied with the conditions mentioned above but for at least 20 min. This caused total removal of polymer from the substrate and deposition of inorganic nanoclusters where the pattern showed the structure induced by photo lithography.

Figure 3 shows a scanning force micrograph of a substrate patterned in such a way. Approximately 8 nm large Au-nanoparticles form a ring where the diameter of the ring resembles the dimension of the photolithographic mask. The separation distance between the particles is approximately 85 nm and corresponds approximately to the separation distances observed in extended monomicellar films (see figure 2(d), table 2).

So far, the pattern geometry is restricted to chains of nanoparticles in suitable configurations dictated by the pre-structure. But photo- or e-beam lithography allows the fabrication of holes in a thin film of a resist with a volume that is comparable to the volume of an individual diblock copolymer micelle with a diameter of 200 nm if dissolved in toluene. E-beam lithography allows rather suitable access to the formation of patterns with dimensions in the range of 50–200 nm. Single micelles were then positioned within these holes through capillary forces as shown in figure 1(c).[5]

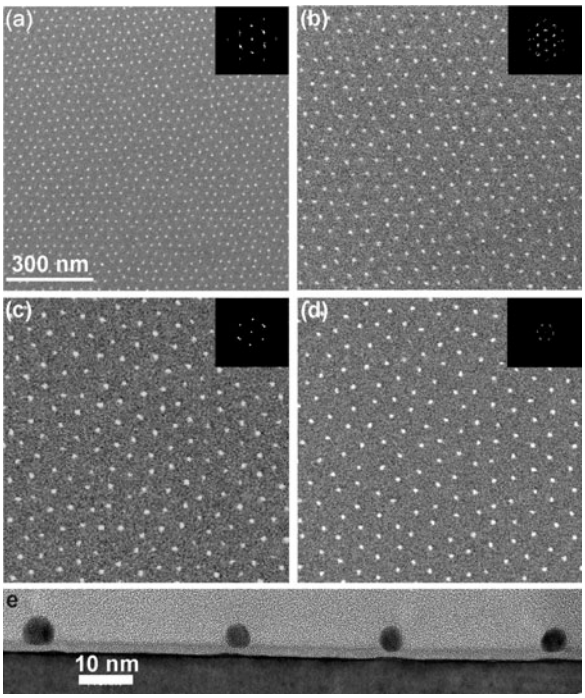

Figure 2. SEM micrograph of Si-wafers structured with Au-nanodots (including fourier transformed images as insets) after hydrogen plasma treatment of monomicellar films prepared from (a) PS(190)-*b*-P[2VP($HAuCl_4$)$_{0.2}$](190), (b) PS(500)-*b*-P[2VP($HAuCl_4$)$_{0.5}$](270), (c) PS(990)-*b*-P[2VP($HAuCl_4$)$_{0.5}$](385), and (d) PS(1350)-*b*-P[2VP($HAuCl_4$)$_{0.5}$](400) micellar toluene solution. (e) Side view transmission electron micrograph of a Si-wafer after embedding it into epoxy and cutting the substrate perpendicular to its surface plane. The brighter layer between the Si(100) and the Au-nanodots displays SiO_2 formed by native oxidation[5].

It is important to realise that the diameter of the micelle (30–200 nm) fits perfectly well with the length scale of e-beam- or even photo-lithography. The single micelle positions its nanoparticle in the centre of the hole [7]. It is the complementary length scale between conventional lithography (photo or e-beam lithography) and self-assembly of associated block copolymers which allows for the generation of actually any pattern size, geometry and also aperiodic structures with rather limited effort.

After formation of e-beam resist pattern and coating of the template with micelles, the substrate is shortly treated with an oxygen plasma and then dipped into acetone for a few seconds to remove the resist film and any micelles deposited on the top surface of the resist. The micelles that were in contact with the substrate, that is inside the holes, remained adsorbed at exactly the position where the hole originally formed. The substrate was finally exposed to oxygen plasma. Figure 4 shows a series of SF-micrographs where the volume of the hole in the resist was systematically reduced by decreasing the resist film thickness from 800, 500 to about 75 nm. The diameter of the

[5] The side view micrograph was provided by PD Dr F Banhard Ulm University, Germany.

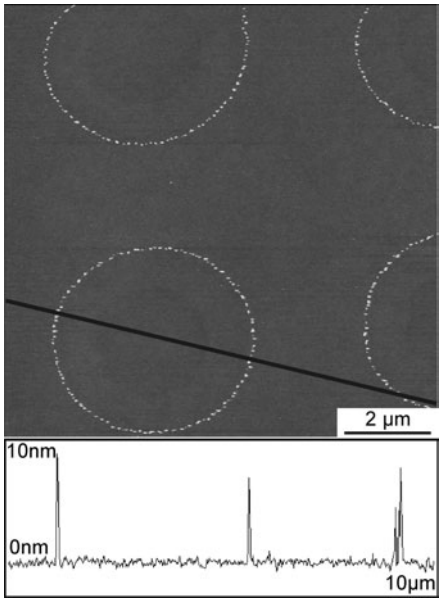

Figure 3. Scanning force microscope images of approximately 8 nm Au-dots that are organized in rings. The ring geometry resembles the pre-pattern generated by standard photo lithography.

hole was approximately 200 nm for all patterns. After lift-off and subsequent plasma treatment Au-nanoparticles resemble the e-beam pattern. With the thicker resist films several Au-nanodots clustered in one spot which is the centre of a previously formed hole in the resist (figures 4(a), (b)). By decreasing the resist thickness to 75 nm only a single 7 nm large Au-nanodot is placed with a localization precision that is comparable to the diameter of the nanoparticle (figure 4(c)).

Nanoscopic lines fabricated by the deposition of spherical micelles along pre-pattern, as shown in figure 3, are not connective. However, variations in the molecular architecture of block copolymers allows access to polymer associates with different morphologies, i.e. spheres, cylinders and vesicles [24–26]. Thus, we use a very valuable fact of diblock copolymer micelles that is the formation of cylindrical micelles.

Cylindrical micelles in solution are formed if the volume fraction of the corona is decreased with respect to volume fraction of the core. It was shown in the case of polystyrene(80)-*block*-poly[2-vinylpyridine(330)] that cylindrical micelles do form upon casting the micellar solution [25]. As in the case of spherical micelles the core block could be neutralized with $HAuCl_4$. Manners *et al* [24, 27] demonstrated in a series of publications stable cylindrical micelle formation of organometallic-inorganic diblock copolymers like poly(dimethylsiloxane)-*block*-poly(ferrocenyldimethylsilane), PDMS-*b*-PFS, in solution.

Cylinders of PDMS-*b*-PFS with a length of several micrometres were deposited onto a resist structured with linear grooves by dip coating [27]. The Si substrate with the structured resist film was dipped into a hexane solution of PDMS-*b*-PFS cylinders and pulled out of the solution with a speed of 5 mm min^{-1}. Figure 5 shows a SF-micrograph of the substrate after the resist film had been removed by immersing the substrate for 30 s into acetone, N_2 flow drying and hydrogen plasma treatment for 10 min at 100 W and 1 mbar hydrogen gas pressure. The image show a SF-micrograph of an aligned nanoscopic lines with a height of about 4 nm. The imaged lateral dimension of the line is convoluted by the tip with the imaged objected. This might allow the fabrication of oriented, nanometre wide electrically active lines of several micrometres in length by a rather low cost method.

2.3. Inorganic-block copolymer micellar monolayers as negative e-beam resist

E-beam lithography is a common method for fabrication of submicron structures. Although a beam of electrons may be focused to <1 nm in diameter, the resolution is limited by the interaction of the beam with the resist material and by the radius of gyration of the macromolecules, which is usually a few nanometres [28]. New developments in using self-assembled monolayers overcome these restrictions inherent with standard resist materials as their thickness is usually a few Angstroms. Structures as small as a few nanometres were fabricated by this concept [15].

In order to locally group a small number of Au-nanoparticles in a designated pattern, extended monomicellar layers are exposed directly to a focused electron beam (e-beam) in a SEM with the idea to chemically modify this particular polymer located in these areas [29][6]. The process is depicted in figure 1(d). In the following experiment, micellar monolayers of PS(990)-*b*-P[2VP($HAuCl_4$)$_{0.5}$](385) on Si-substrates were processed with an e-beam at 1 keV. The electron doses ranged between 400 and 50 000 μC cm^{-2}. The exposed areas resemble the structures of squares and stars with a minimal width of 200 nm, which is the width of the electron beam. Then, the locally exposed layers were washed in a dimethylformamide (DMF) or toluene ultrasound bath[7] for 5 min. The SEM micrograph in figure 6(a) shows block copolymer micelles on a Si-substrates after lift-off of non-irradiated micellar monolayers. Non-irradiated areas are rather perfectly freed from polymer while areas of the micellar monolayers that were irradiated by the e-beam show the same micellar pattern as before the e-beam exposure and lift-off step. In order to deposit Au-nanoclusters from these films onto the Si-wafer, the substrate was exposed to a hydrogen plasma (150 W, 0.4 mbar, 30 min). Figure 6(b) shows the same star shaped structured marked by 7 nm large Au-dots. The Au-dot pattern is similar to figure 2(d) but Au is only found in the areas where the e-beam exposed the micellar monolayer. Thus, this techniques also allows for the generation of rather complex nanostructures.

The e-beam writing on micellar structures with 10 kV and electron doses ranging from 400 to 50 000 μC cm^{-2} resulted in almost the same polymer pattern as writing with 1 kV for the pattern demonstrated in figure 6(a). However most of the micelles did not seem to contain any gold. After plasma treatment, no Au nanoclusters could be detected. Since higher electron energies reduce the radius of cross section between

[6] For electron-beam lithography of the coated silicon substrates the FE-SEM was used in combination with a beam-blank-controller (Raith) including the Software (Raith Nanolithography System, Version 2.07).

[7] To remove non-irradiated areas from the solid interface DMF p.a. from Merck or toluene p.a. from Acros were used in combination with ultrasound bath (Bandelin Sonorex Super RK102h).

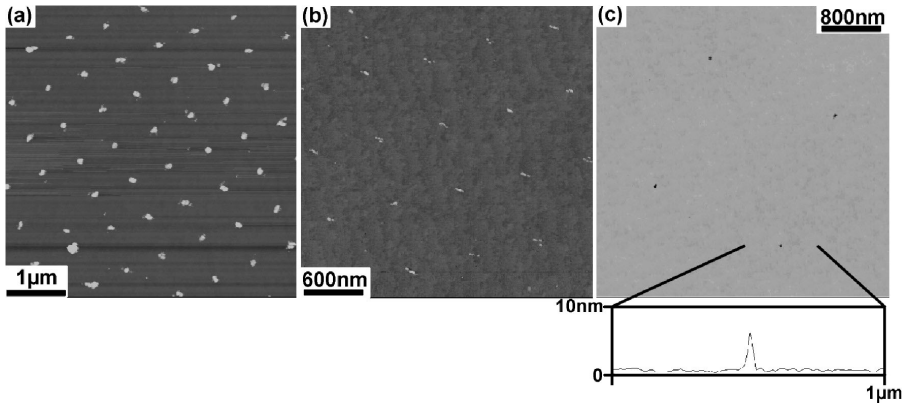

Figure 4. SF-micrographs shown here depict deposition of Au-nanoclusters after lift-off of the e-beam resist. The resist contained holes of 200 nm diameter, while varying film thickness from (a) 800 nm, (b) 500 nm, (c) 75 nm in order to control the volume of the hole. SF-micrographs vary according to the volume of the holes and show (a) cluster made of several Au-nanodots, (b) up to four individual Au-nanodots and (c) single 7 $\pm$ 0.5 nm large Au-clusters. The clusters are separated from each other by 2 μm forming a square lattice pattern. The contrast of the last image has been inversed for improved visualization. The height profile of a line which is running over an individual Au-cluster is indicated underneath showing the folding of the SFM-tip with the cluster geometry.

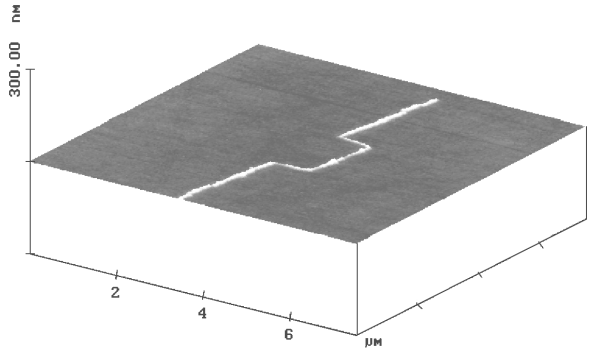

Figure 5. SF-micrograph showing a continuing 4 nm wide line after the oriental deposition of PDMS-*b*-PFS diblock copolymer cylinders along pre-patterned grooves of a resist film, lift-off of the resist with acetone and subsequent hydrogen plasma treatment.

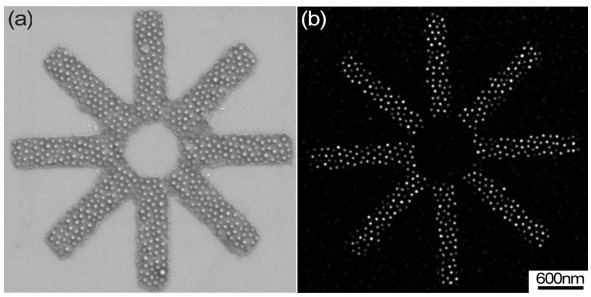

Figure 6. Scanning electron micrographs of (a) a monomicellar layer after lifting-off the non electron exposed micelles and (b) after the hydrogen plasma treatment, which deposited 7 nm large Au-nanoparticles in a star pattern.

the electron and the polymer, we propose that in the case of 10 kV exposure, the chemical modification of the polymer was not sufficient for stabilizing the Au in the micelles during the lift-off process. DMF is a stronger lift-off solvent than toluene, but less selective. In the case of smaller electron doses, DMF treatment caused removal of the crosslinked polymer micelles, while toluene did not.

The limit in the number of Au-nanoclusters per pattern area is shown in figure 7. Here, the electron exposed area was systematically reduced down to 100 $\times$ 100 nm^2 in figure 7(f). The projected profile of the focused e-beam determines the area of the polymer in the micellar monolayer that is crosslinked upon interaction with electrons. Despite the size of the e-beam, the beam profile may not cover the area of a single micelle at the edge of a pattern fully. These micelles are either lifted-off fully because of weak crosslinking due to small electron doses ($<$1000 μC cm^{-2} at 1 keV) or by insufficient exposure of the micellar area by the e-beam. The solvent partly removes polymer, $HAuCl_4$ and Au seeds that are associated to P2VP segments from the cores of micelles. As observed by SFM, the heights of Au-clusters at the edges can vary from 1 nm up to the 7 nm, the height of Au-clusters observed in the centre of patterns.

X-ray photoelectron spectroscopy (XPS) demonstrated the chemical modification of the polymer upon electron exposure due to oxidation of polystyrene and polvinylpyridine, which results in the formation of carboxylic acids, ketones, aldehydes and ethers associated to the polymer. Such results are reported in [30] when the electron irradiated polymer layer was exposed to air. The formation of these carbon species and their chemical interaction with Si–OH on the substrates strongly supports that electron exposed diblock copolymer micelles are stabilized at the Si-wafer due to this modifications.

The application of monomicellar films as negative e-beam resist is another demonstration to create 'micron nanostructured' patterns marked by uniform nanoclusters. The match of two different length scales, i.e. self-assembly of block copolymers ($<$100 nm) and e-beam writing ($>$50 nm) allows one to group nanometre-sized clusters at very small numbers in periodic or aperiodic patterns and to separate these groups by length scales which are not accessible by pure self-assembly. The sizes of the clusters are much smaller than could be obtained with other lithographic techniques. The molecular weights of the diblock copolymers and the loading of the micellar solutions with $HAuCl_4$ control particle size and particle-to-particle distance on the nanometre scale. The area of the e-beam controls the micron length scale, i.e. the separation of groups of Au-nanoparticles as well as the number of nanoparticles per group.

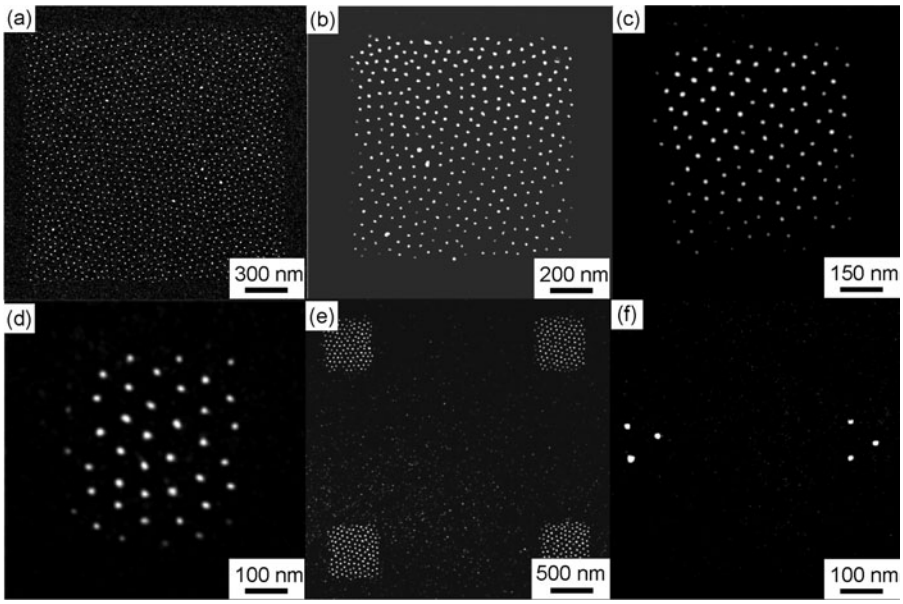

Figure 7. SEM-micrographs of groups of Au-nanodots after e-beam exposure, lift-off and hydrogen plasma treatment. Each structure is marked by ∼7 nm large Au-clusters which are separated by approximately 73 nm: (a) $2 \times 2\ \mu m^2$, (b) $1 \times 1\ \mu m^2$, (c) $0.5 \times 0.5\ \mu m^2$, (d) $250 \times 250\ nm^2$, (e) $0.5 \times 0.5\ \mu m^2$ squares separated by $2\ \mu m$, and (f) a pair of three densely packed Au-dots where the pairs are separated by 400 nm.

2.4. Guided self- assembly of block copolymer micelles on electrical isolating substrates

Generation of nanostructures is an important issue in applications related to optical microscopy. In biology, for example, optical transparent glass cover slips are preferable substrates through which biological matter is imaged by inverted optical microscopes. The deposition of extended nanodot pattern on glass cover slips as described in section 2.1 is straightforward. The same applies for guided self-assembly in the case when pre-structures are prepared by photo lithography. However, features which need the application of electron beam lithography as shown in section 2.3 require a conductive substrate such as a Si-wafer which is not transparent in the visible light range. However, most of optical transparent substrates are electrical isolating. Coating glass substrates with indium–tinoxide (ITO) makes them conductive, does not change its optical transparency tremendously but changes the surface chemistry and makes the surface very rough. This roughness is in the range of typical 10–20 nm which distorts the precise fabrication of nanostructures.

In order to overcome this limitation an approximately 5 nm thick layer of carbon is evaporated on top of a monomicellar film on a glass cover slip as shown schematically in figure 8(a). The roughness of this layer was less than 1 nm and it is sufficient conductive to apply the underlying monomicellar film as negative e-beam resist as described in section 2.3. Finally, the carbon was removed with the polymer layer by the gas plasma treatment.

Figure 8(b) shows a monomicellar layer on glass after successful lift-off of micelles that are not irradiated by the e-beam. Micelles are arranged in squares. Figure 8(c) depicts 7 nm large Au nanoparticles on glass. The fact that this process was done on glass cover slips is recognized by the small holes (marked by arrows) which are characteristic for glass cover slips.

2.5. Mechanical stability of nanopattern

The nanopattern reported here are formed by the assembly of Au-clusters on different substrates. Other cluster materials, such as Ag, AgO_x, Pt, Pd, ZnO_x, TiO_x, Co, Ni, or FeO_x are possible as well. Especially in the case of Au, the question arises concerning nanopattern's mechanical stability. Contrary to evaporated or sputtered gold layers on glass or silicon substrates, which easily can be removed by touching the layer with a rather soft tissue or in an ultrasonic water bath, these nanopattern demonstrate enormous mechanical stability. Substantial chemical treatments with 'Piranha' acid, different bases, alcohols or water does not affect the pattern. This pattern's mechanical stability have opened many different approaches which are currently under investigation, e.g., regarding its application in biology as templates for immobilizing single proteins and probing their interactions with living cells or as coatings for lenses and filters [31]. Pattern's thermal treatment up to 800 °C have shown no cluster mobility or coalescence. But it resulted in Au evaporation from clusters which did not affect the cluster's position. We assume that this remarkable mechanical stability which is essential for future's application is well-founded in the plasma processes described above as the polymer removal step. Also O_2-, H_2-, or Ar-plasma application does not affect SFM the cluster supporting substrates substantially, displayed slight substrate roughening. This leads to the hypothesis that the edge formed by the substrate–cluster borderline is partly wetted by surface atoms of the substrate activated by the plasma process. This argument is underlined by SFM images of $SrTiO_3$ substrates from where Au-clusters have been dissolved by KJ. These images display very small dips with a depth of ∼0.5 nm at former positions of Au-clusters as demonstrated in figure 9. Thus, we assume that the mechanical stability of the clusters on the substrates results from lateral stabilization of the clusters by a very thin aggregation of substrate atoms at the edge of

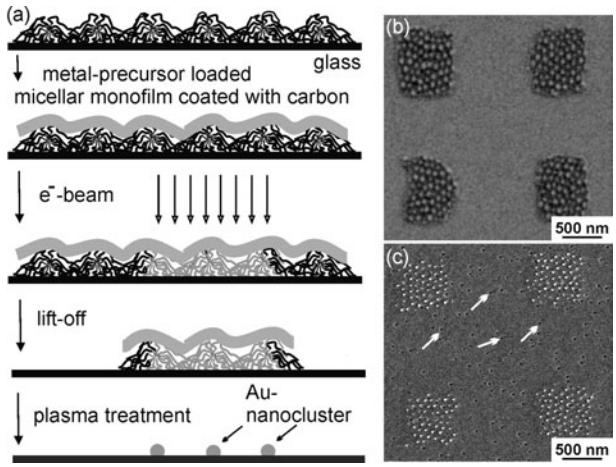

Figure 8. Application of monomicellar films as negative e-beam resist on glass cover slips. (a) Schematic drawing, (b) monomicellar layers after lift-off and (c) Au-nanodots of 7 nm diameter after hydrogen plasma treatment. The white arrows point to holes which are characteristic for glass cover slips.

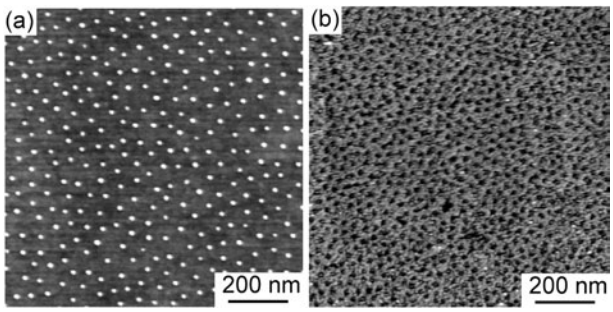

Figure 9. SFM image of (a) Au-nanoclusters deposited from PS(1700)-*b*-P[2VP($HAuCl_4$)$_{0.5}$](400) onto $SrTiO_3$; (b) the same substrate than in (a) but after dissolving nanoparticles by KJ [32].

the substrate–cluster borderline due to the plasma process. This is also confirmed by observations of varying mechanical stability of Au-clusters on different substrates since the plasma affects chemical different substrates with different strength. Au-clusters have been moved with less force applied from an scanning force microscope probe if deposited on $SrTiO_3$ than on glass or Si substrates where cluster movement have been rather impossible. This substrate dip which stabilizes individual clusters might be also reflected from the HRTEM image shown in figure 2(e). An additional hypotheses is based on the formation of alloys between the cluster and the substrate material. e.g. Au forms alloys with Si. Yet, the role of this for mechanical stability of patterns has not been confirmed.

3. Conclusion

Block copolymer micelle nanolithography is demonstrated to be a suitable and easy accessible technique to generate nanostructured interfaces. The nanostructures consist of dots or lines. The pattern dimension and geometry is controlled by the combination of the self-assembly of block copolymer micelles with pre-structures formed by photo or e-beam lithography. Thus, a large variety of rather complex structures can be designed which will be of interest for different fields, such as nanoelectronics or bio-nanotechnology.

Acknowledgment

The Deutsche Forschungsgemeinschaft supported this work in the frame of the Gerhard-Hess programme (SP 520).

References

[1] Ozin G A 1992 *Adv. Mater.* **4** 612
Antonietti M and Göltner C 1997 *Angew. Chem. Int. Edn* **36** 910
[2] Beginn U and Möller M 1999 Supramolecular structures with macromolecules *Supramolecular Technology* vol 4, ed D N Reinhoudt (New York: Wiley) ch 3
[3] Beginn U 1998 *Adv. Mater.* **10** 1391
[4] Alivisatos P, Barbara P F, Castleman A W, Chang J, Dixon D A, Klein M L, McLendon G L, Miller J S, Ratner M A, Rossky P J, Stupp S I and Thompson M E 1998 *Adv. Mater.* **10** 1297
[5] Spatz J P 2002 *Angew. Chem. Int. Edn.* **114** 3359
[6] Moore G E 1965 *Electronics* **38** 114
[7] Spatz J P, Chan V Z-H, Mößmer S, Möller M, Kamm F-M, Plettl A and Ziemann P 2002 *Adv. Mater.* **24** 1827
[8] Deng T, Ha Y-H, Cheng J Y, Ross C A and Thomas E L 2002 *Langmuir* **18** 6719
[9] Xia Y, Rogers J A, Paul K E and Whitesides G M 1999 *Chem. Rev.* **99** 1823
Xia Y, Rogers J A, Paul K E and Whitesides G M 1999 *Chem. Rev.* **99** 1641–990 (series of articles)
[10] Lee K B, Park S J, Mirkin C A, Smith J C and Mrksich M 2002 *Science* **295** 1702
Hong S, Zhu J and Mirkin C A 1999 *Science* **286** 523
[11] Park M, Harrison C K, Chaikin P M, Register R A and Adamson D A 1997 *Science* **276** 1401
[12] Rockford L, Liu Y, Mansky P, Russell T P, Yoon M and Mochrie S G J 1999 *Phys. Rev. Lett.* **82** 2602
[13] Morkved T L, Lu M, Urbas A M, Ehrichs E E, Jaeger H, Mansky P and Russell T P 1996 *Science* **273** 931
[14] Boneberg J, Burmeister F, Schäfle C, Leiderer P, Reim D, Fery A and Herminghaus S 1997 *Langmuir* **13** 7080
[15] Gölzhäuser A, Eck W, Geyer W, Stadler V, Weimann T, Hinze P and Grunze M 2001 *Adv. Mater.* **13** 806
[16] Yang X M, Peters R D, Kim T K, Nealey P F, Brandow S L, Chen M-S, Shirey L M and Dressick W J 2001 *Langmuir* **17** 228
[17] Wyrwa D, Beyer N and Schmid G 2002 *Nano Lett.* **2** 419
[18] Lin X M, Parthasarathy R and Jaeger H M 2001 *Appl. Phys. Lett.* **78** 1915
[19] Lammertink R G H, Hempenius M A, van den Enk J E, Chan V Z-H, Thomas E L and Vancso G J 2000 *Adv. Mater.* **12** 98
[20] Böltau M, Walheim S, Mlynek J, Krausch G and Steiner U 1998 *Nature* **391** 877
[21] Spatz J P, Sheiko S and Möller M 1996 *Macromolecules* **29** 3220
[22] Spatz J P, Mößmer S and Möller M 1996 *Chem. Eur. J.* **2** 1552
[23] Spatz J P, Mößmer S, Möller M, Herzog T, Boyen H G, Ziemann P and Kabius B 2000 *Langmuir* **16** 407
[24] Massey J A, Power K N, Winnik M A and Manners I 1998 *J. Am. Chem. Soc.* **120** 9533
[25] Spatz J P, Mößmer S and Möller M 1996 *Angew. Chem. Int. Edn Engl.* **35** 1510
[26] Zhang L, Yu K and Eisenberg A 1996 *Science* **272** 1777
[27] Massey J A, Winnik M A, Manners I, Chan V Z H, Ostermann J H, Enchelmaier R, Spatz J P and Möller M 2001 *J. Am. Chem. Soc.* **123** 3147
[28] Gibson J M 1997 *Phys. Today* **50** 56
[29] Glass R, Arnold M, Blümmel J, Küller A, Möller M and Spatz J P 2003 *Adv. Funct. Mater.* **13** 569
[30] Onyiriuka E C 1994 *J. Adhes. Sci. Technol.* **8** 1
[31] Arnold M, Cavalcanti-Adam A, Glass R, Blümmel J, Eck W, Kessler H and Spatz J P 2003 submitted
[32] Thomas Herzog *PhD Thesis* Ulm University, Germany